

Lessons from TRMM and Plans for GPM

Arthur Y. Hou

NASA Goddard Space Flight Center, Greenbelt, Maryland, USA

1. Introduction

The TRMM satellite has been in orbit for approximately 3 years and is expected to continue for another 2 to 3 years. TRMM has been a tremendous success in demonstrating the combined use of active and passive microwave sensors to provide high-quality precipitation observations from space. Since its launch in November 1997, much progress has been made in sensor calibration, ground-based validation, and satellite algorithm improvement. TRMM rainfall data are now being used in a wide range of applications and scientific research. I will focus on three issues: First, how accurate are the TRMM rainrates? Second, how useful are TRMM data? Third, how can we do better with GPM?

Section 2 is a brief review of the Tropical Rainfall Measuring Mission (TRMM). Section 3 gives the status of current TRMM rainfall products and validation activities. Section 4 shows a few examples of TRMM science results. Section 5 discusses the use of TRMM rainfall retrievals in weather forecasting and data assimilation. Section 6 reports on the status of the Global Precipitation Mission (GPM) and highlights the crucial role of international partnership in making GPM a reality.

2. Background

TRMM was initially conceived as a highly-focused, limited-objective program aimed at measuring the monthly and seasonal rainfall over 10^5 km² in the tropics and subtropics (Simpson 1988). Its goals are to understand the global water and energy cycles by providing a quantitative description of the tropical rainfall and latent heating, and to understand the mechanisms by which tropical heating influences the global climate. Unlike the SSM/I instruments on DMSP satellites, TRMM was designed to collect information about the diurnal variability of tropical rainfall. It was also the first to use a space-borne precipitation radar as a flying rain gauge to cross-calibrate rainfall estimates derived from passive radiometer and infrared (IR) sensors, with the ultimate goal of providing a long-term rainfall analysis based on combined space-borne sensors.

Standard TRMM data products are made available to the general science community through NASA's Goddard Distributed Active Archive Center (DAAC) within 72 hours of collection. Even though providing rainfall data for the prediction of weather and climate is a key TRMM objective from the very beginning, the TRMM near real-time system was not created till the post-launch phase primarily due to cost concerns. It was ultimately made possible by delivering data in near real-time on a best-effort basis rather than as an operational requirement. The TRMM near real-time system provides TRMM rainfall retrievals within 3 hours of collection of the oldest byte of data in orbit (which reflects that TRMM observations are downlinked once per 90-minute orbit). TSDIS currently provides TRMM near real-time data to more than a dozen forecast centers around the globe.

While the overarching goal of TRMM is to improve the understanding of the hydrological cycle and its role in the global climate, TRMM was not designed to provide the final answer. TRMM is flying in a precessing,

low-inclination (35°), and low-altitude (350 km) orbit in order to achieve high spatial resolution and capture the diurnal variation of tropical rainfall. With a single satellite, the sampling and coverage are inevitably limited at short time scales. However, before launching a fleet of rainfall satellites, it is essential to demonstrate the viability and utility of space-based rainfall measurements. TRMM was meant to provide that demonstration and build consensus satellite algorithms for future missions.

The TRMM rain sensor package consists of (1) a conical-scanning 13.8 GHz precipitation radar (PR) with 4.3 km footprint, 0.25 km vertical resolution, and a 215 km swath; (2) a cross-tracking, multi-frequency (10.7, 19.3, 21.3, 37.0, and 85.5 GHz), dual-polarized (except for 21.3 GHz, which is vertical-only) microwave radiometer (TMI), with a 10 x 7 km field of view at 37 GHz, and a 760 km swath; and (3) an infrared and visible scanner (VIRS) with 0.63, 1.61, 3.75, 10.8, and 12 μm at 2.2 km resolution and a 720 km swath (see Fig. 1). The PR provides detailed information on the 3D rain structure and convective/stratiform (C/S) rain types. The VIRS senses the cloud-top radiances. The purpose of VIRS is to enable TRMM to establish the connection between microwave and geostationary IR-based rain measurements. Details of TRMM rain sensors may be found in Kummerow et al. (1998). An example of simultaneous images from PR, TMI and VIRS is shown in Fig. 2.

TRMM Rain Sensors: PR, TMI, and VIRS

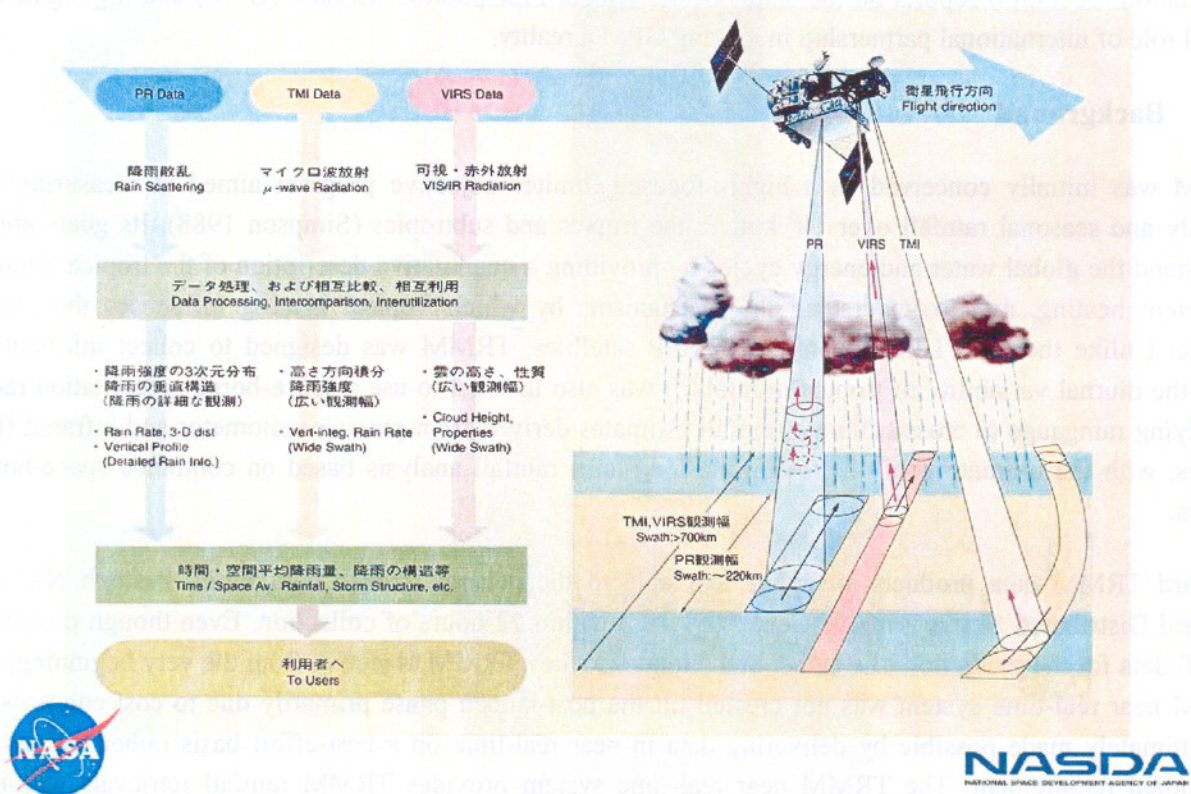


Fig 1. A schematic of the three TRMM rain sensors: PR, TMI, and VIRS.

Simultaneous PR, TMI, and VIRS Images

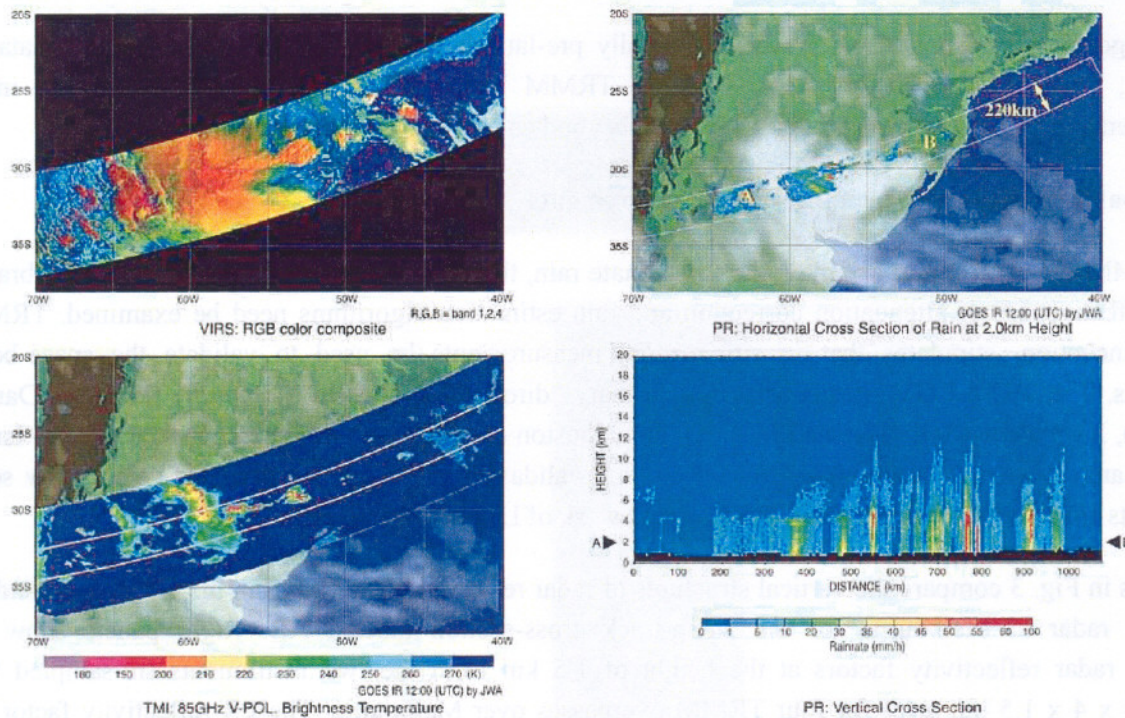


Fig 2. Simultaneous PR, TMI, VIRS images superimposed with GEOS IR images. IR and visible sensors observe cloud-top radiances, while microwave instruments are capable of providing information beneath the clouds.

In addition to the rain package, the TRMM satellite carries two related EOS instruments, the Clouds and the Earth's Radiant Energy System (CERES) and Lightning Imaging Sensor (LIS), to round out its science mission. The LIS instrument (Goodman et al. 1996) observes the frequency of global lightning events and provides a link between lightning occurrences and precipitation events. The CERES instrument (Wielicki et al. 1996) measures the radiation in infrared and shortwave spectra, which together with the latent heating estimates derived from precipitation can provide a better understanding of the atmospheric energy balance.

3. Validation of TRMM Version 5 Rainfall Products

The validation plan for TRMM satellite rainfall products calls for two ground segments. The first consists of a number of carefully-calibrated ground validation (GV) sites around the world to provide ground radar and rain-gauge measurements as independent checks of TRMM satellite data. The second consists of a series of field campaigns with aircraft undeflights to provide microphysical information to validate and improve

satellite retrieval algorithms and cloud physical models. TRMM GV and field campaign data are collected and distributed through the Goddard DAAC to the science community.

TRMM algorithm Versions 1 and 2 were essentially pre-launch test codes. The current TRMM data are Version 5, introduced on October 1, 1999. The TRMM Version 5 algorithms incorporate the initial improvements in the first two years after its launch, beyond corrections of software errors.

3.1. Comparison of PR with ground radar measurements

Since TRMM PR is the first airborne radar to estimate rain, the accuracy and stability of the PR calibration and the effectiveness of attenuation correction and rain estimation algorithms need be examined. TRMM, from its inception, stipulates that *in situ* ground measurements be used to validate the space-borne instruments. The TRMM GV sites consist of 4 primary “direct data” sites in Melbourne (Florida), Darwin (Australia), Kwajalein Atoll (Marshall Islands), and Houston (Texas), with additional special sites in Israel, Brazil, Guam, Taiwan, Thailand and Hawaii. Ground validation is an ongoing activity. I will show some early results from the Melbourne radar, based on the work of Liao and Meneghini (2001).

Left panels in Fig. 3 compare the vertical structures of radar reflectivity derived from the TRMM PR and the WSR-88D radar at Melbourne for the along-track cross-section labeled AB. Right panels show the coincident radar reflectivity factors at the height of 1.5 km from the two instruments (re-sampled to a common 4 x 4 x 1.5 km grid) for four TRMM overpasses over Melbourne. The PR reflectivity factor has been corrected for attenuation effects. The good agreement between the two instruments is evident in the scatter plots and reflectivity histograms (lower panels). The averaged correlation coefficient is 0.89 for a total of 24 overpass cases over Melbourne in 1998.

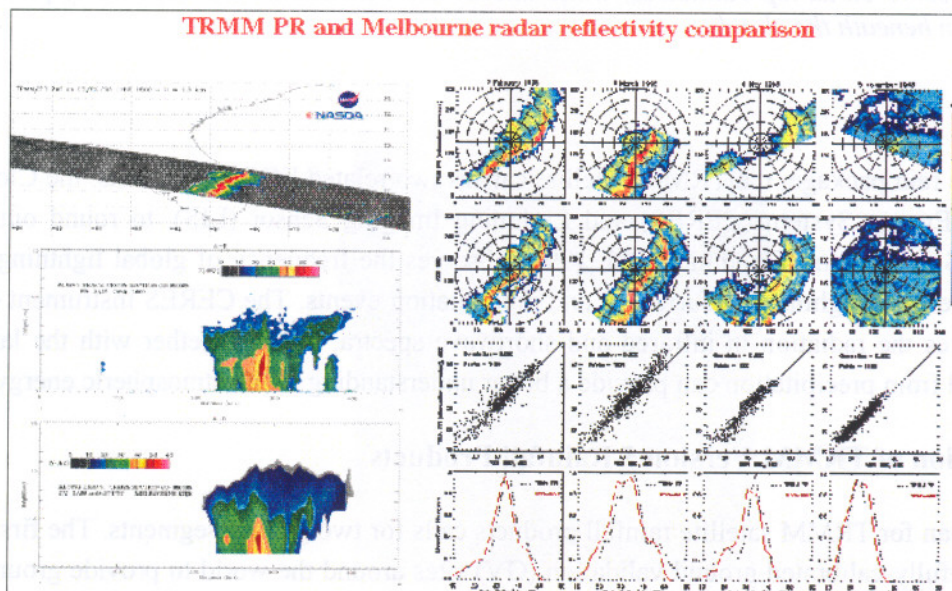


Fig 3. Comparison of attenuation-corrected PR reflectivity at 1.5 km with ground radar measurement at Melbourne, FL.

In terms of rainrates, Fig. 4 shows that the agreement is quite good considering that the PR and GV radar algorithms use different Z-R relationships and different convective/stratiform classifications. Notwithstanding such differences, the statistics of the 24 overpasses in 1998 yield a correlation coefficient of 0.873 for the pixel-averaged rainrates. The correlation coefficient improves to 0.95 for the area-averaged rainrates, with a mean rainrate of 1.25 mm/h for PR and 1.21 mm/h for the Melbourne radar.

As already mentioned, the PR and GV radar use different structural information of the reflectivity field for C/S classifications. The PR relies on the presence of bright bands to detect stratiform rain. In the absence of a well-defined bright band it reverts to a more standard algorithm based on the horizontal structure, similar to that use by ground radars. Interestingly, despite the different C/S classifications, there is a good quantitative agreement in the percentage convective rain between the PR and GV radars, as shown in Fig. 4. The agreement in rainrates and rain-types is encouraging but must be regarded as tentative since the calibration of the Melbourne radar against raingauges varies significantly from month to month, which requires further investigation.

Comparison of rainrates derived from TRMM PR and GV radar at Melbourne

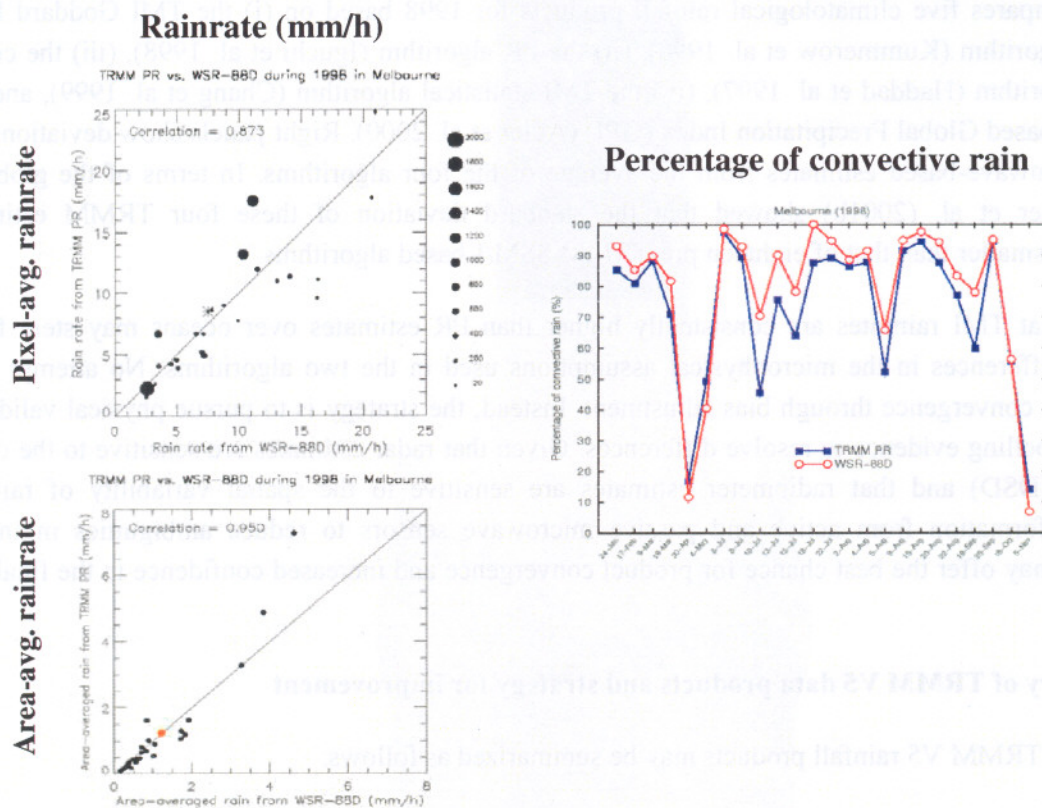


Fig 4. Comparison of rainrates derived from PR and GV radar for 24 TRMM overpasses in 1998 at Melbourne. In the figure for the pixel-averaged rainrates, the size of the circle is proportional to the number of pixels in each overpass.

Elsewhere, comparisons of satellite data with gauge rainrates show a sizable range of discrepancies. The work of Adler et al. (2001b) showed biases of -1%, -31%, and -17% for the monthly TMI, PR and combined

PR/TMI algorithms against Pacific atoll gauges. As the validation effort progresses, there is an increasing recognition that there is no easy “ground truth” since gauges and GV radars can have as much uncertainty as satellite retrievals. Much work is needed to reduce uncertainties arising from data gaps, Z-R relations, calibration errors, rain-type classifications, and errors of representativeness. Since ground measurements and physical validation serve different purposes in validation, what is needed is a mix of high-quality conventional raingauge data to provide sanity checks, plus field campaigns to provide coordinated microphysics-microwave measurements.

3.2. Intercomparison of V5 satellite rain products

Figure 5 compares the instantaneous rainrates derived from the PR and TMI. Left panels show surface rainrates during Hurricane Floyd on 13 September 1999. The right panel is a scatter plot of surface rainrates in dBR for all coincident raining pixels averaged for August 1998. At small rainrates, the TMI shows a high bias relative to the PR, which is reflected in the ratio of TMI to PR rainrate for stratiform rain (see Table in Fig. 5), while the PR has a high bias in the convective rainrate relative to the TMI. But, averaged over the global tropics and subtropics, the TMI estimate is greater than the PR rainrate by about 20%.

Figure 6 compares five climatological rainfall products for 1998 based on (i) the TMI Goddard Profiling (GPROF) algorithm (Kummerow et al. 1996), (ii) the PR algorithm (Iguchi et al. 1998), (iii) the combined PR-TMI algorithm (Haddad et al. 1997), (iv) the TMI statistical algorithm (Chang et al. 1999), and (v) the adjusted IR-based Global Precipitation Index (GPI) (Adler et al. 2000). Right panels show deviations of four TRMM microwave-based estimates from the average of the four algorithms. In terms of the global-mean rainrate, Adler et al. (2001b) showed that the standard deviation of these four TRMM estimates is significantly smaller than that of eighteen pre-TRMM SSM/I-based algorithms.

The result that TMI rainrates are consistently higher than PR estimates over oceans may stem from the systematic differences in the microphysical assumptions used in the two algorithms. No attempt is being made to seek convergence through bias adjustment. Instead, the strategy is to pursue physical validation by seeking compelling evidence to resolve differences. Given that radar estimates are sensitive to the drop size distribution (DSD) and that radiometer estimates are sensitive to the spatial variability of rain, using combined information from active and passive microwave sensors to reduce ambiguities in individual instruments may offer the best chance for product convergence and increased confidence in the final rainfall estimates.

3.3. Summary of TRMM V5 data products and strategy for improvement

The status of TRMM V5 rainfall products may be summarized as follows:

- The satellite and GV data are in excellent agreement in identifying “rain” or “no rain” at the pixel scales. For instance, comparisons at Kwajelein show that the satellite and GV estimates disagree only in 13 out of 283 cases.
- The TRMM V5 satellite rainfall products are within 20% in terms of zonal averages, 24% for tropical monthly averages, and 30-50% bias in instantaneous rainrates.

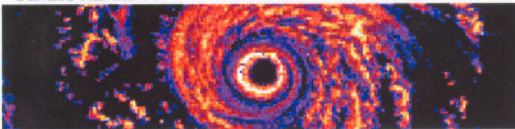
- The uncertainty among V5 satellite algorithms is comparable to the difference between satellite and ground-based estimates.
- There is no easy “ground truth” since gauges and radars can have as much uncertainty as satellite retrievals. These include uncertainties in data gaps, Z-R relations, calibration errors, rain-type classifications, and errors of representativeness. We need to use a mix of high-quality conventional rain gauge data to provide sanity checks, plus field campaigns to provide coordinated microphysics-microwave measurements.
- Further agreement between the space-borne and ground-based sensors will require a better understanding of precipitation physics using knowledge gained from TRMM experiments (TEFLUN-A/B, SCSMEX, TRMM-LBA, and KWAJEX). Justifiable modifications of algorithms must be done in the context of physical validation (i.e., validating the physics of algorithms, not just the rainrates).
- Convergence to a global-mean bias of 10-15% in monthly mean rainrates is a reasonable goal for Version 6.

PR and TMI instantaneous rainrate comparison

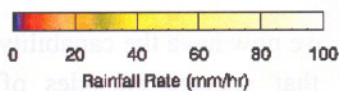
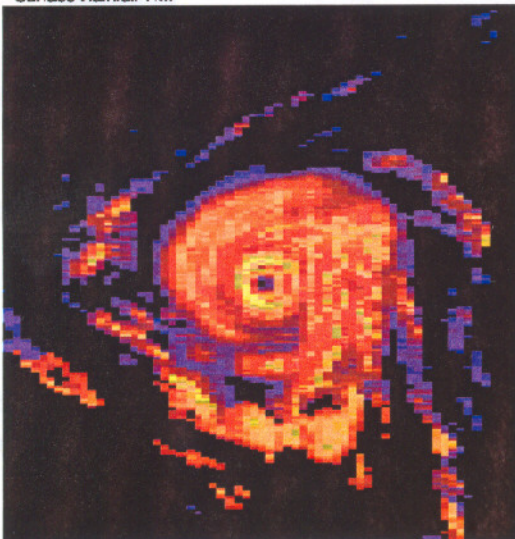
Hurricane Floyd 135 knots

990913/0930Z V5

Surface Rainfall PR



Surface Rainfall TMI



August 1998 OCEAN

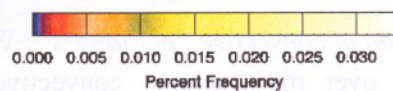
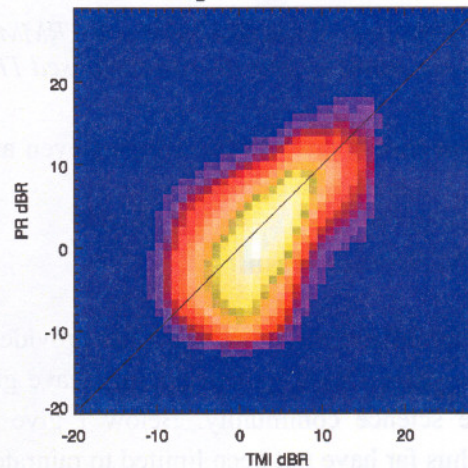


Fig 5. Comparison of instantaneous rainrates derived from TRMM PR and TMI.

Rainfall climatology from different algorithms

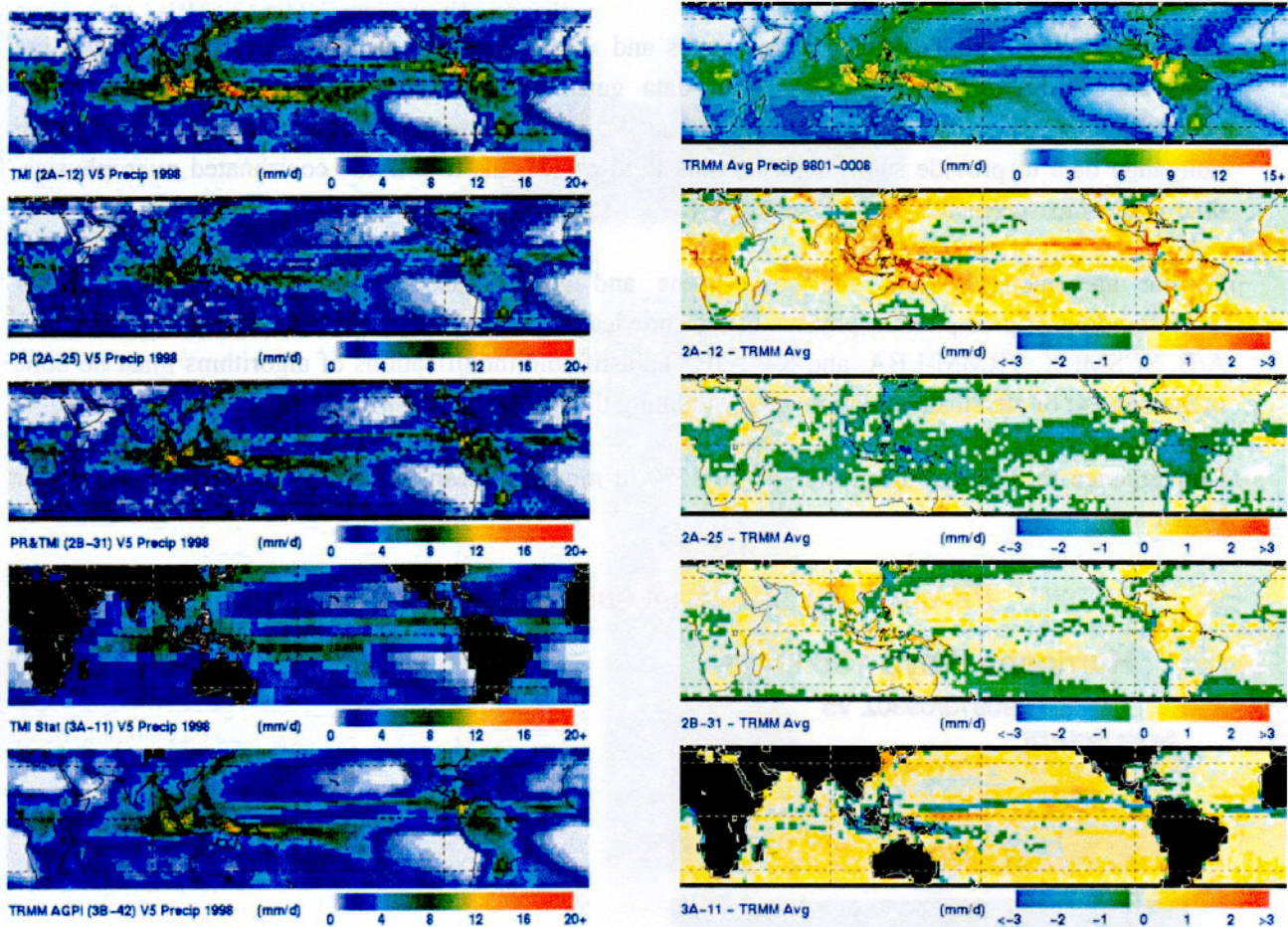


Fig 6. Left panels: Comparison of five TRMM climatological rainfall products for 1998. Right panels: Deviations of four microwave-based TRMM algorithms from the average of the four.

In Section 5, we show that TRMM rainrates even at their current level of accuracy are still useful in data assimilation and numerical weather prediction.

4. TRMM Science Results

In addition to rainfall estimation, TRMM has provided a wealth of information in broader scientific contexts. In the past few years TRMM science results have generated much interest and excitement in the media as well as in the science community. Below I give a few examples as a reminder that TRMM science contributions thus far have not been limited to rainrate estimation.

Direct observation of convective “hot towers”: With TRMM PR, we now have the capability to observe - on a routine basis over the tropics - convective “hot towers” that presage episodes of rapid cyclone intensification. An example of hot towers from Hurricane Bonnie is shown in the top panel in Fig. 7. These giant “chimney” clouds in the eyewalls of intensifying cyclones typically tower to 17-18 km, overshooting into stratosphere, and are part of a mesoscale (100-200 km) phenomena known as convective outbursts.

These are long-lived (several hours) aggregates of eyewall convection and often presage episodes of rapid intensification. The hypothesis is that these events represent diluted convection bringing air with high equivalent potential temperature from the tropical boundary layer to the upper-troposphere in the inner core region. The subsequent release of latent heat could then lead to the rapid intensification. TRMM data have been used to study latent heat release associated with these chimney clouds and convective outbursts (Simpson et al. 1998, Halverson et al. 1999).

TRMM science results

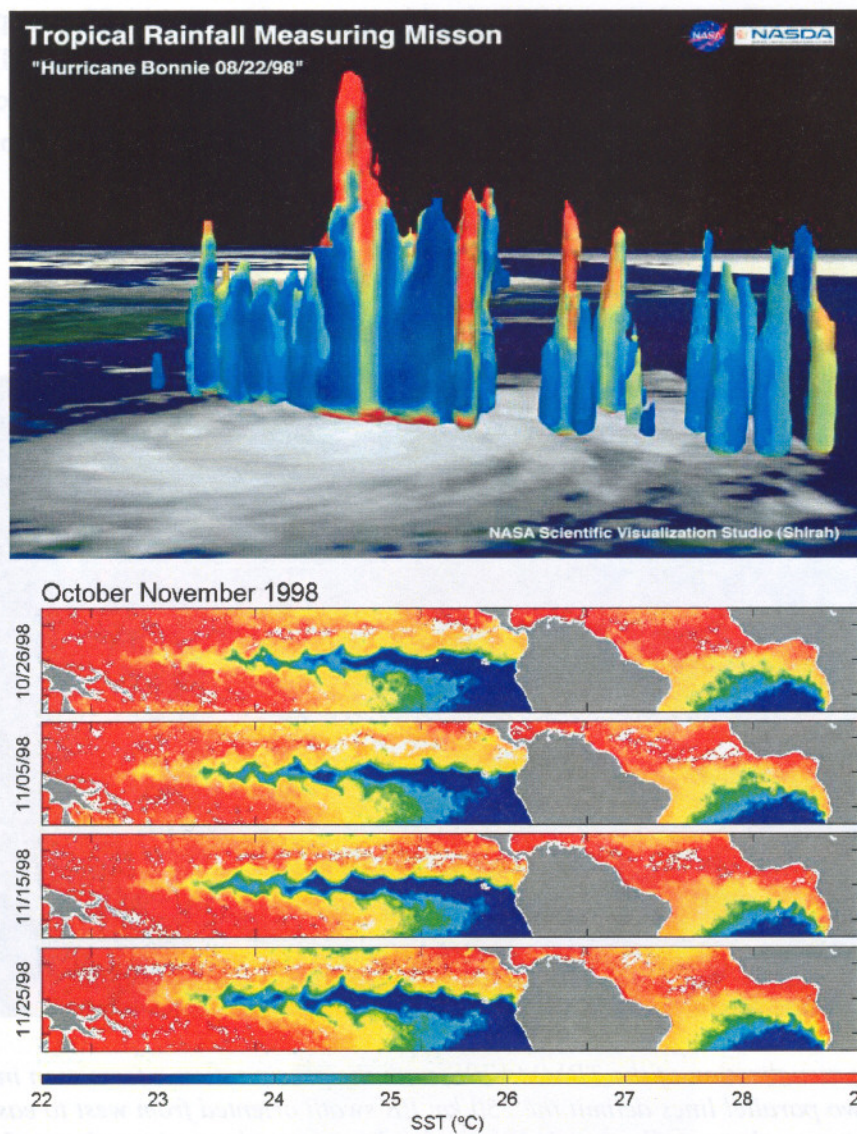


Fig 7. Examples of TRMM science results. Top: Direct observations of chimney clouds in Hurricane Bonnie. Bottom: TMI SST measurements through clouds.

Sea-surface temperature measurement (SST) through clouds: TMI provides high-resolution SST measurements through clouds. Unlike IR instruments, it permits nearly uninterrupted monitoring of the ocean surface in all weather conditions (except rain). TMI also provides simultaneous retrievals of SST and

surface wind speed, ideal for surface flux studies. During Hurricanes Bonnie and Danielle in late August 1998, TMI data showed that the intensity of Danielle weakened as it crossed the cold wake produced by Bonnie (Wentz et al. 2000). This cold wake was hidden by clouds in the SST field derived from AVHRR. TMI SST data also provided early detection of the 1998 La Niña and observations of instability waves on the interface between the cold South Equatorial current and warm counter-currents on either side over the eastern tropical Pacific Ocean (lower panel in Fig. 7).

Suppression of rain and snow by smoke and air pollution: Simultaneous TRMM PR, TMI, and VIRS observations provided direct evidence showing that urban and industrial air pollution inhibits precipitation over southeastern Australia. Figure 8 shows VIRS cloud image superimpose with PR precipitation (in white overlay). A pollution plume with smaller drop sizes is visible in box 2, as indicated in yellow. TRMM PR only detected rain in the unpolluted clouds in boxes 1 and 3. The VIRS-retrieved effective radius data confirm that the largest cloud droplet in the polluted clouds is below the 14 μm precipitation threshold (Rosenfeld 2000).

TRMM science results

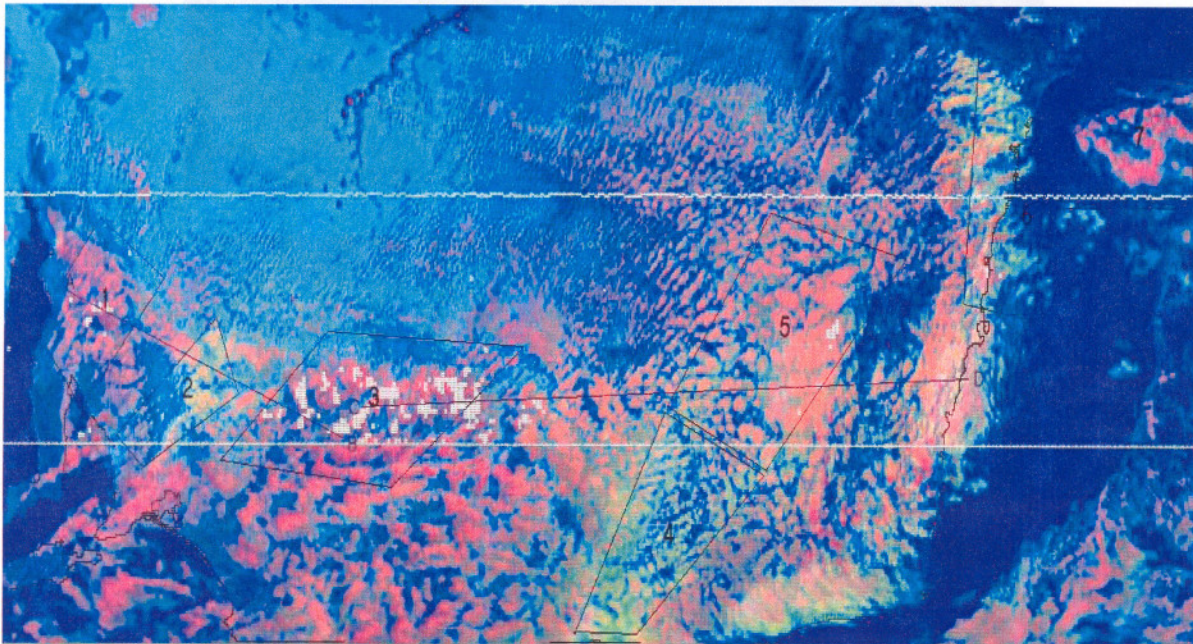


Fig 8. Satellite visualization of the TRMM VIRS, with the precipitation information in the white overlay. The two parallel lines delimit the 230 km PR swath oriented from west to east (i.e., left to right). The image shows pollution plumes in clouds over southeast Australia on 21 October 1998 at 04:44 UT (copyright: AAAS, reproduced from Rosenfeld, 2000, with the author's permission.)

5. Use of TRMM Rainfall Retrievals In Global Modeling And Data Assimilation

As discussed in Section 3, at the present time rainrates retrieved from microwave sensors have enough uncertainties to provide but an estimate of the truth. Given such uncertainties, it is reasonable to ask whether TRMM rainfall products are useful in global data assimilation and weather forecasting. The answer depends upon whether TRMM rainrates are in some sense better than estimates generated by the parameterized moist physics in global models. Since absolute validation of rainrates is difficult, one must rely on practical metrics to evaluate the impact of rainfall assimilation in global forecasting and data assimilation systems. Recent studies at ECMWF, FSU, and NASA have all shown positive impact in using TRMM rainfall data in global applications with different assimilation techniques and evaluation metrics. The benefits range from improved tropical precipitation and cyclone forecasts to improved clouds and radiation in data analyses (Krishnamurti et al. 2000, Marecal and Mahfouf 2001, Hou et al. 2001). However, the impact of TRMM rainrates on forecast and analysis can vary with the manner by which they are assimilated. Given the reality that parameterized convection will likely remain less than perfect for some time, there is a need to explore new methodologies to make more effective use of microwave-based rainrates in data assimilation.

Global analyses currently contain significant errors in the primary hydrological fields such as precipitation, evaporation (WCRP 1998). The discrepancies are especially pronounced in the tropics, where conventional observations are sparse and assimilated rainfall data are based largely on model estimates, which are sensitive to the parameterized physics used in the model. We also know that the convective schemes used in global models are not perfect. Errors in convective parameterizations can lead to substantial systematic errors in forecast. However, forecast biases are generally not treated in conventional analysis schemes, which could cause useful observations being rejected. The underlying assumption in data assimilation is that the first-guess fields and forward models are not biased. But, in the case of precipitation assimilation, this assumption is severely challenged, especially at locations where TRMM microwave instruments (which are excellent rain detectors) sense rain but the model does not produce rain.

With this in mind, at NASA Goddard we have performed assimilation experiments using TMI and SSM/I rainfall retrievals to explore the potential of using microwave-based rainfall observations to compensate for errors in physical tendencies in the Goddard Earth Observing System (GEOS) Data Assimilation System (DAS), following a strategy similar to that outlined in Derber (1989). The scheme we developed is a variational procedure based on a 6-h integration of a column model of moist physics with prescribed dynamic and other physical tendencies (Hou et al. 2000). It produces temperature and/or moisture tendency corrections to compensate for the total tendency error arising from model deficiencies and initial conditions. This variational procedure in space and time, in its generalization to 4 dimensions, is related to the standard 4D-Var scheme but estimates temperature and/or moisture tendency corrections instead of modifying the initial conditions.

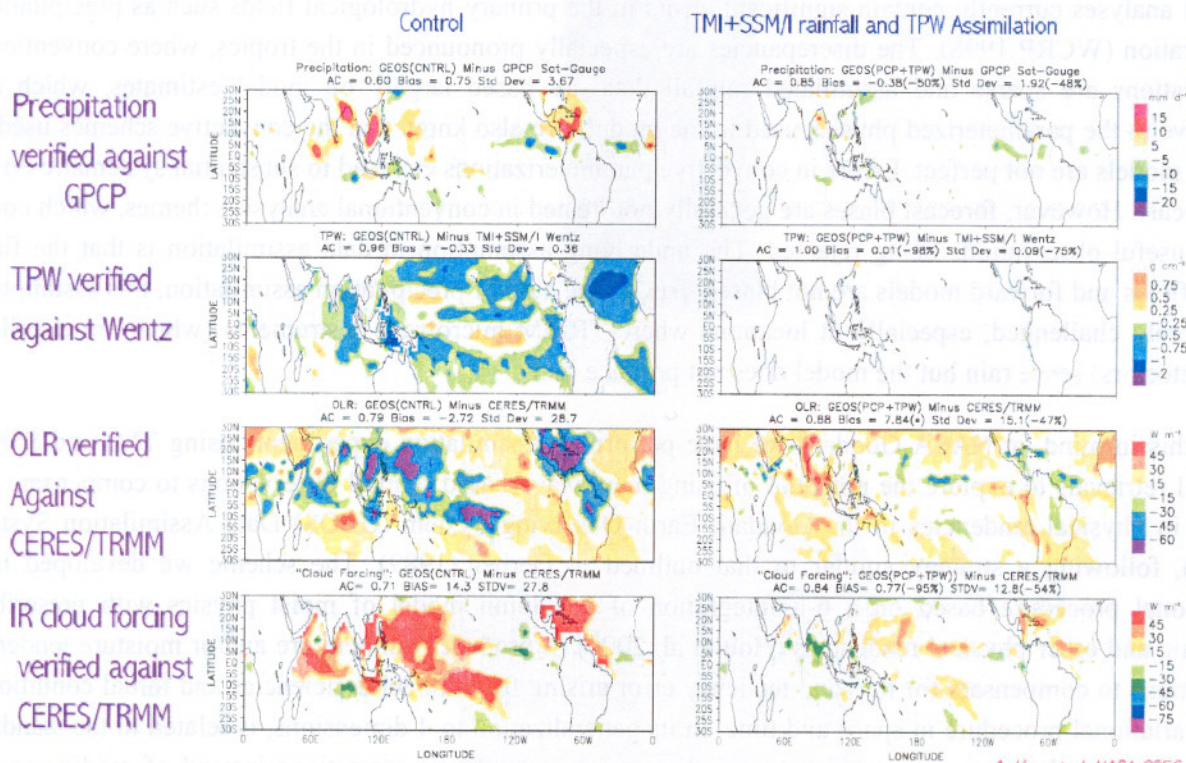
Figure 9 shows that assimilating TMI and SSM/I rainrates and TPW improves not only the hydrological cycle but also key climate parameters such as cloud and radiation, as verified against the independent CERES (ERBE-like) OLR measurements. Analysis shows that rainfall assimilation using the tendency correction approach effectively reduces state-dependent systematic errors in the assimilation fields. Ensemble forecasts show that the improved analysis also leads to better short-term tropical forecasts of the

geopotential height at 500 hPa, divergent winds at 200 hPa, and precipitation (see Hou et al. 2001 for details).

The above results suggest that in assimilating precipitation, for which the forward model is based on parameterized physics, it may be important to develop assimilation techniques that recognize model biases to realize the full benefit of observations. In practice, the tendency correction procedure described here may be incorporated in a standard 4D-Var scheme. Ultimately, it may be possible to improve model physics by using information in these tendency corrections to diagnose state-dependent systematic model errors, as outlined in DelSole and Hou (1999).

The main point of this section is to remind us that the usefulness of precipitation data in data assimilation depends not only on the accuracy of the observation but also on how the data are assimilated.

Impact of rainfall assimilation on the GEOS Analysis



A. Hou et al. NASA GSFC

Assimilation of satellite-based rainfall data improves clouds and TOA radiation.

Fig 9. NASA GEOS assimilation results with and without TMI and SSM/I observations for June 1998. Left panels show errors in the monthly-mean tropical precipitation, total precipitable water, outgoing longwave radiation, and IR cloud forcing in the GEOS control assimilation. Right panels show the impact of assimilating TMI and SSM/I rainfall and TPW observations on these fields. Percentage changes relative to errors in the GEOS control are given in parentheses.

6. International Partnership and Formulation of GPM

I would like to begin the discussion of GPM with the recognition that international collaboration has played a crucial role in making TRMM a success. Even though TRMM began its life as a joint U.S.-Japan mission, EuroTRMM has made significant contributions. They range from fundamental research on surface cross-sections for PR attenuation correction, to improvement of TMI rain products using coincident PR data, working with NASDA to assess PR algorithms, providing inputs to the designing of the TRMM real-time data products, and application of TRMM data in numerical weather forecasting, as described in other articles in this workshop. The success of this international partnership has provided a key cornerstone for the GPM.

Building upon the success of TRMM, the Global Precipitation Mission is a multinational satellite project to improve current precipitation knowledge and to extend rainfall measurements to higher latitudes. Within NASA, GPM is part of systematic measurements within the Earth Science Enterprise Strategic Plan to improve understanding of the global water and energy cycle. The reference concept of the GPM consists of two primary space segments, as shown in Fig. 10. The core satellite is to carry a dual-frequency, precipitation radar, a multi-frequency radiometer flying in a non-Sun synchronous orbit with an inclination greater than 60° . The goal of the core satellite is to improve understanding of precipitation structure and physics, and to provide calibrations for the constellation radiometers.

The GPM Reference Concept 2 Primary Space Segments

CORE SATELLITE

- Dual frequency radar
- Multifrequency radiometer
- Non-sun synchronous orbit
- $\sim 60^\circ$ inclination
- $\sim 400 - 500$ km altitude

MISSION: Understand rainfall structure and provide training for constellation radiometers.

Notionally 3 hourly sampling



CONSTELLATION SATELLITES

- 8 small satellites with radiometer only*
- 3 hr revisit time
- Sun-synchronous polar orbit
- ~ 600 km altitude
- Some of the 8 small satellites can be replaced by existing radiometers (i.e., SSSMs, AMSR, etc.)

MISSION: Provide enough sampling to reduce uncertainty in short-term rainfall accumulations. Scientific and societal applications.

Near real-time data processing & dissemination

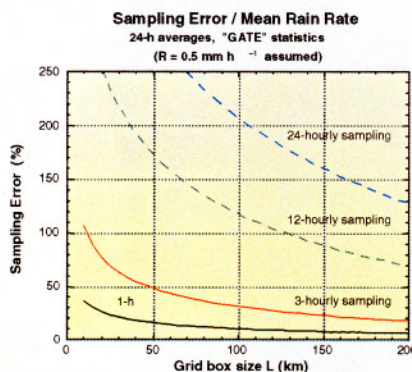


Fig 10. The GPM reference concept and estimated sampling errors in daily rainrate as functions of the grid-box size and the satellite revisit time.

The second segment is a constellation of eight small, radiometer-only satellites placed in Sun-synchronous polar orbits. It is envisioned that some members of the constellation can be existing radiometers such as DMSP's SSM/Is and NASDA's GCOMB-1/AMSR. The constellation radiometers are to provide, in near real-time, near-global coverage and frequency sampling to reduce uncertainties in short-term rainfall estimates. The GPM reference concept is based on notionally 3 hourly sampling with 8 constellation radiometers. Shown in Fig. 10 is an estimate of the sampling error in daily rainrate as functions of the grid-box size and satellite revisit time based on GATE data (Bell 2001). The final configuration of these space segments will be determined by a trade-space study based on GPM science requirements.

NASA has just received the legislative authority to proceed with the formulation of GPM to define requirements, examine options, and define partnerships. The GPM is conceived as a truly international partnership, its success will require developing effective partnerships between individual scientists, NASA, NASDA, ESA, and other international and sister U.S. agencies. The coming years promise to be an exciting time when the international partners work together to transform the GPM vision into reality.

Acknowledgments

It is a pleasure to acknowledge the support of this work by Dr. Ramesh Kakar, the TRMM Program Scientist at NASA Headquarters. I would like to thank my TRMM colleagues, Bob Adler, Tom Bell, Tricia Gregory, Chris Kummerow, Bob Meneghini, Bill Olson, John Stout, Jeff Halverson, Lisa Harold, Marshall Shepherd, Arlindo da Silva, Eric Smith, Erich Stocker, Dave Wolff, and Sara Zhang, for generous contributions and assistance in preparing this overview, Frank Wentz for permission to use the TMI SST image in Fig. 7, and Daniel Rosenfeld for permission to use the VIRS/PR image in Fig. 8.

References

- Adler, R. G. Huffman, D. Bolvin, S. Curtis, and E. Nelkin, 2000: Tropical rainfall distributions determined using TRMM combined with other satellite and raingauge information, *J. Appl. Meteor.*, **39**, 2007-2023.
- Adler, R. C. Kidd, G. Petty, M. Morrissey, M. Goodman, 2001a: Intercomparison of global precipitation products: The Third Precipitation Project (PIP-3). *Bull. Amer. Meteor. Soc.*, **82**, 1377-1396.
- Alder, R., C. Kummerow, D. Bolvin, S. Curtis, and C. Kidd, 2001b: Status of TRMM monthly estimates of tropical precipitation. *Meteorological Monographs: Symposium for Joanne Simpson and TRMM*, submitted.
- Bell, T., P. Kundu, and C. Kummerow, 2001: Sampling errors of SSM/I and TRMM rainfall averages: Comparison with error estimates from surface data and a simple model. *J. Appl. Meteor.*, **40**, 938-954.
- Chang, A., L. Chiu, C. Kummerow, and J. Meng, 1999: First results of the TRMM Microwave Imager (TMI) monthly oceanic rain rate: Comparison with SSM/I. *Geophy. Res. Letters*, **26**, 2379-2382.
- Delsole, T., and A.Y. Hou, 1999: Empirical correction of a dynamic model: Part I. Fundamentals. *Mon. Wea. Rev.*, **127**, 2533-2545.
- Derber, J.C., 1989: A variational continuous assimilation technique. *Mon. Wea. Rev.*, **117**, 2437-2446.
- Goodman, S. J., et al., 1996: The optical transient detector: First results. Preprints, *Eighth Conf. On Satellite Meteorology*, Atlanta, GA, Amer. Meteor. Soc., 583-587.
- Haddad, Z., E. Smith, C. Kummerow, T. Iguchi, M. Farrar, S. Durden, M. Alves, and W. Olson, 1997: The TRMM "Day-1" radar/radiometer combined rain-profiling algorithm. *J. Met. Soc. Japan*, **75**, 799-809.
- Halverson, J., H. Pierce, J. Simpson, C. Morales, and E. Rodgers, 1999: First TRMM satellite observations of deep convective outburst in super-typhoon Paka. *Proc. 23rd Hurricane and Tropical Meteorology*, Dallas, TX, 997-1000.
- Hou, A.Y., D. Ledvina, A. da Silva, S. Zhang, J. Joiner, R. Atlas, G. Huffman, and C. Kummerow, 2000: Assimilation of SSM/I-derived surface rainfall and total precipitable water for improving the GEOS analysis for climate studies. *Mon. Wea. Rev.*, **128**, 509-537.
- Hou, A.Y., S. Zhang, A. da Silva, W. Olson, C. Kummerow, and J. Simpson, 2001: Improving global analysis and short-range forecast using rainfall and moisture observations derived from TRMM and SSM/I passive microwave sensors. *Bull. Amer. Meteor. Soc.*, **82**, 659-680.
- Iguchi, T., T. Kozu, R. Meneghini, J. Awaka, and K. Okamoto, 1998: Preliminary results of rain profiling with the TRMM precipitation radar. *Proc. 8th URSI Com F Triennial Open Symposium, "Wave Propagation and Remote Sensing"*, Aveiro Portugal, 147-150.

- Krishnamurti, T., C. Kishtawal, T. LaRow, D. Bachiochi, Z. Zhang, C. Williford, S. Gadgil, and S. Surendran, 2000: Multi-model superensemble forecasts for weather and seasonal climate. *J. Climate*, **13**, 4196-4216.
- Kummerow, C., W. Olson, and L. Giglio, 1996: A simple scheme for obtaining precipitation and vertical hydrometer profiles from passive microwave sensors. *IEEE Trans. Geosci. Remote Sens.*, **34**, 1213-1232.
- Kummerow, C., W. Barnes, T. Kozu, J. Shiue, and J. Simpson, 1998: The Tropical Rainfall Measuring Mission (TRMM) sensor package. *J. Atmos. Oceanic Tech.*, **15**, 809-817.
- Liao, L., and R. Meneghini, 2001: Comparison of rain rate and reflectivity factor derived from the TRMM precipitation radar and the WSR-88D over the Melbourne, FL site. *J. Atmos. Oceanic Tech.*, submitted.
- Marecal, V., and J.-F. Mahfouf, 2001: 4D-Var assimilation of TMI rainfall rates. *Proc. ECMWF/EuroTRMM Workshop on Assimilation of Clouds and Precipitation*, ECMWF, 6-9 November 2000 (this issue).
- Rosenfeld, D., 2000: Suppression of rain and snow by urban and industrial air pollution. *Science*, **287** (10 March), 1793-1796.
- Simpson, J. (Ed.), 1988: *TRMM: A Satellite Mission to Measure Tropical Rainfall*. Report of the Science Steering Group. NASA Publications, U.S. Government Printing Office, Washington, D.C. 94pp.
- Simpson, J., J. Halverson, H. Pierce, C. Morales, and T. Iguchi, 1998: Eying the eye: Exciting early stage science results from TRMM. *Bull. Amer. Meteor. Soc.*, **79**, 1711.
- Wentz, F., C. Gentemann, D. Smith, and D. Chelton, 2000: Satellite measurement of sea-surface temperature through clouds. *Science*, **288** (5 May), 847-850.
- Wielicki, B. A., et al., 1996: Clouds and the Earth's Radiant Energy System (CERES): An earth observing system experiment. *Bull. Amer. Meteor. Soc.*, **77**, 853-868.
- World Climate Research Program (WCRP), 1998: *Proc. First WCRP International Conference on Reanalyses*, Silver Spring, MD, WCRP, 461 pp.

APPENDIX: Acronyms

AAAS	American Association for the Advancement of Science
AVHRR	Advanced Very High Resolution Radiometer
CERES	Clouds and the Earth's Radiant Energy System
C/S	convective/stratiform
DAAC	Distributed Active Archive Center
DAS	data assimilation system
DSD	drop size distribution
DMSP	Defense Meteorological Satellite Program
ECMWF	European Centre for Medium-Range Weather Forecasts
ERBE	Earth Radiation Budget Experiment
ESA	European Space Agency
FSU	Florida State University
GATE	Global Atmospheric-Research-Program Atlantic Tropical Experiment
GEOS	Goddard Earth Observing System
GPCP	Global Precipitation Climatology Project
GPM	Global Precipitation Mission
GV	ground validation
KWAJEX	Kwajalein Experiment
TRMM-LBA	TRMM-Large Scale Biosphere-Atmosphere Experiment in Amazonia
LIS	Lightning Imaging Sensor
NASA	National Aeronautics and Space Agency
NASDA	National Space Development Agency (of Japan)
OLR	outgoing longwave radiation
PR	Precipitation Radar
SCSMEX	South China Sea Monsoon Experiment
SSM/I	Special Sensor Microwave/Imager
TEFLUN	Texas-Florida Underflight Experiment
TMI	TRMM Microwave Imager
TOA	top-of-the-atmosphere
TPW	total precipitable water
TRMM	Tropical Rainfall Measuring Mission
TSDIS	TRMM Science and Data Information System
VIRS	infrared and visible scanner
WCRP	World Climate Research Program